Journal of Fluids and Structures (2000) **14,** 1195–1214
doi:10.1006/jfls.2000.0314, available online at http://www.idealibrary.com on IDEAL®

AQUEOUS FLOW LIMITATION IN A TAPERED-STIFFNESS COLLAPSIBLE TUBE†

C. D. Bertram and W. Chen

Graduate School of Biomedical Engineering, University of New South Wales Sydney, Australia 2052

(Received 18 March 1999, and in final form 28 March 2000)

To find out whether the relation between flow-limited flow-rate and upstream transmural pressure was nonunique, as has been reported for air flow through a tapered-stiffness tube, and for comparison with a completed investigation of flow limitation in a uniform tube, flow limitation was observed in a tapered-stiffness tube. The tube was made by removal of material from the outside of a segment of the previous uniform tubing; thus the stiffness was on average less than that of the uniform tube. Therefore, quantitative differences in behaviour were expected, but in addition significant qualitative differences were found. Whereas in the uniform tube, large-amplitude oscillations were almost entirely confined to a transition from peak pre-collapse flow-rate to the largely pressure-drop-independent flow-limited flow-rate, the latter state here included operating points of all oscillatory types. The dramatic reduction in flow-rate at the transition was absent, and instead multiple (up to six) operating points occurred at a single value of upstream head and upstream transmural pressure. The plotting of control–space diagrams revealed a unique region of weak oscillations corresponding to the tube throat being located at an intermediate and time-varying point along the tube, with collapse as far as that point only. These oscillations were extremely variable in waveshape and frequency, often displayed intermittency, and depended sensitively on the precise operating point conditions. When in this mode, the tube upstream of the final collapse position exhibited small standing waves of area, so that up to four just-perceptible minima were seen.

1. INTRODUCTION

In an extended series of experiments, Bertram and colleagues have investigated the dynamics of relatively thick-walled uniform silicone-rubber collapsible tubes undergoing flow-induced oscillations. The pressure-drop/flow-rate characteristics and oscillatory modes were mapped under conditions of pressure-drop limitation, when the downstream transmural pressure is held constant (Bertram 1986a; Bertram *et al.* 1990). A new concept, the control-space diagram, was introduced for the systematic analysis of these data as a function of tube length and downstream resistance (Bertram *et al.* 1991). The constitutive relationship between transmural pressure and tube cross-sectional area in the absence of flow was established by Bertram (1987). In order to understand the possible extent of interactions with the rest of the recirculating flow system, the frequency-dependent input impedance up- and downstream of the tube was characterized and varied by Bertram and Butcher (1992). Detailed profiles along the tube of instantaneous internal cross-sectional area and pressure during flow-induced oscillation were measured (Bertram *et al.* 1994; Bertram and Godbole 1995). Most recently, the pressure-drop/flow-rate characteristics were re-examined under conditions of flow-rate limitation, when the upstream transmural

† Presented in part at the 3rd World Congress of Biomechanics, Sapporo, Japan, August 2–8, 1998.

0889–9746/00/111195 + 20 $35.00/0

pressure is held constant (Bertram and Castles 1999). It was found that these tubes exhibit an exaggerated degree of flow-rate reduction as they enter the flow-limited state. While the relationship between upstream transmural pressure and flow-limited flow-rate was monotonic, at least for a given direction of transmural pressure change, the range of such flow-limited flow-rates was small and the flow-rates themselves were small, relative to the maximum flow-rate reached before the tube collapsed and the flow-limited state was attained. The transition, from the maximum pre-limitation flow-rate to the value that was independent of pressure drop along the tube, traversed those regions of tube behaviour control-space where large-amplitude oscillations occurred. Once past this transition, oscillations were largely absent; thus flow limitation itself was not associated with self-excited oscillation. [Flow limitation without oscillation was also observed by Gavriely *et al.* (1989). The idea of this association goes back at least to Brower and Scholten (1975), who found the outbreak of spontaneous oscillations to coincide with the fluid speed reaching the (critical) pressure wave speed. This is the choking condition of gas dynamic analogy, which Griffiths (1969) used to explain flow limitation in the collapsible urethra. Conversely, the idea that oscillations require this fluid speed has also been undermined. Grotberg and Gavriely (1989) showed theoretically that instabilities leading to flutter could arise at lower fluid speeds, and Yamane and Orita (1992) observed subcritical oscillations at low downstream resistance.]

Meanwhile, Kamm and colleagues were investigating the properties of tapered-stiffness collapsible tubes, i.e. tubes in which the wall thickness increases in the streamwise direction. Such tubes are arguably a better model of the collapsible conduits in the respiratory system, at least when breathing out. In a student thesis, subsequently reported in a conference abstract (Kamm *et al.* 1993), they found evidence that the widely accepted notion that flow-limited flow-rate is determined uniquely by upstream transmural pressure was not true for tubes of such tapering stiffness. When the flowing fluid was air, as many as three quite widely separated flow-rates could be set up at the one value of upstream transmural pressure. However, this behaviour was not found when the flow was aqueous.

In a tube with sufficiently rapidly increasing stiffness in the streamwise direction, in contrast to the situation in a uniform tube, the position where the collapse is abolished is no longer the downstream end where the tube is supported, but an intermediate one (Shapiro 1977). Thus the throat position becomes a new dynamic variable, and new system properties, such as those found by Kamm *et al.* (1993), are to be expected. In view of the potential significance of these alterations, we have investigated thoroughly the pressure-drop/flow-rate characteristics of a tapered-stiffness tube, with particular respect to its flow-rate limitation behaviour. We find a number of important qualitative differences between the uniform and the tapered tube.

2. METHODS

Our apparatus for recirculating aqueous fluid through a collapsible tube has been detailed in the series of papers from this laboratory referred to in the Introduction, so only a brief exposition will be given here. Because the tubes we work with have rather greater wall thickness relative to radius than those traditionally investigated, the pressures needed to bring about the full range of dynamical behaviour potentially available are greater than can be conveniently accommodated through hydrostatic head. We therefore use a recirculating flow system involving two pumps and compressed air pressurisation (Bertram 1986b) to set accurately constant adjustable upstream head conditions.

Approximately following procedures devised at MIT (Kamm *et al.* 1991), the tapered-stiffness tube was created by machining a uniform tube mounted on a mandrel in a lathe.

The tube was of silicone rubber, 267 mm long, with nominal diameters $\frac{1}{2}$ in (12·7 mm) internally and $\frac{11}{16}$ inch (17·46 mm) externally. It was first eased onto the purpose-built solid metal mandrel, then dipped in liquid nitrogen until frozen, then mounted between centres above a trough which loosely encircled the mandrel at each end of the tube. The purpose of the trough was to catch liquid nitrogen and form a shallow pool into which the tube wall dipped at every rotation. Liquid nitrogen was continuously poured onto the tube during the machining process from a nozzle held in a fixed position relative to the lathe cutting tool. The taper was formed by offsetting the tailstock position laterally away from the tool, so that the minimum wall thickness occurred at the headstock chuck. Two cuts were made to reach the final dimensions; lighter cuts and more passes tended to cause a bad surface finish. The nitrogen flow-rate was adjusted to keep the tube at a temperature low enough that the silicone rubber was hard but not so low that it was glassy. The tool was advanced using the slowest thread-cutting rate available on the lathe. The whole lathe area was vigorously ventilated by fans and open windows to minimize the risk of undiluted nitrogen gas being inhaled by the lathe operator. After machining, the tube was left mounted on the mandrel and thawed in water, then eased off. The final tube dimensions were as follows: the taper started approximately 39 mm from the downstream end of the tube segment, and progressed linearly over 210 mm to a minimum outside diameter of 14·1 mm (representing a wall thickness of 0·7 mm), before the tube reverted to original outside diameter for the furthest upstream 16 mm. As eventually mounted in the pressure chamber (on perspex pipes of i.d. 12·1 mm, o.d. 14·3 mm), the unsupported length between the rigid pipes was 228 mm, so that the unsupported tube segment ended with some 18 mm of uniform original tubing. Longitudinal tension in the mounted segment was set as previously for uniform tubes, by fixing the tube at the length it adopted when turned vertically and supporting the axial load provided by a hanging 0·32 kg mass. This implies an increasing strain towards the thin-walled end of the tube, and a higher axial strain on average than was used with the uniform tube. In all other respects the experimental conditions corresponded to those used by Bertram *et al.* (1990, 1991); the resistance to flow in the apparatus downstream was set to the lowest of the three values used then.

The pressure–area relation was measured at 11 locations along the tapered segment, using the conductance catheter method (McClurken 1978; Bertram 1987) to measure local shape-independent tube cross-sectional area. The liquid filling of the tube was at atmospheric pressure, so that negative transmural pressure was the positive air pressure in the chamber around the tube, measured by an accurate gauge pressure indicator (Wallace and Tiernan). The conductance catheter electrodes were 1·4 mm long, spaced 0·9 mm apart on a catheter of diameter 1·3 mm which ran through the whole tube, exiting the system at each end beyond the pressure chamber via a gland in a specially constructed curved section of rigid pipe. To avoid interfering with the collapse, the catheter was arranged so that it lay in one of the two patent tear-drop-shaped lobes left after local collapse to the point of opposite-wall contact. Bertram (1987) showed that the method succeeds in transducing correctly the total tube cross-sectional area under these conditions.

The protocol for the experiments with flow was as established by Bertram and Castles (1999). First, a control-space diagram was established for each direction of external pressure movement. Our control space has the axes p_u (constant flow-driving head pressure, far upstream) and $\bar{p}_{e2} = p_e - \bar{p}_2$, where p_e is the constant pressure in the pressure chamber external to the tube, and $\bar{p}_2$ is the time-mean of the pressure measured at the downstream end of the tube. This space is investigated by systematic variation of p_e at various different p_u levels. The data ultimately allow partition of the whole space into closed regions, each corresponding to a different mode of behaviour. Separate diagrams for increasing and for decreasing p_e are necessitated by hysteresis in the dynamical behaviour.

Then, the flow-limitation behaviour was investigated at a series of constant values of $\bar{p}_{e1} = p_e - \bar{p}_1$, where p_1 is the pressure measured at the upstream end of the tube. For each such constant-$\bar{p}_{e1}$ curve, a standard series of six p_u-values (13, 33, 66, 100, 133 and 166 kPa) was investigated, giving nominally six points on the curve, but in practice often more because of multiple points (see Section 3). For uniform tubes, in order to find precisely the start and end points of the transition to (or from, in the case of the set of curves for reducing p_e) flow limitation, Bertram and Castles investigated further points between those on either side of the transition, incrementing or decrementing p_u by 1 kPa at a time. Here, because of the prevalence of multiple points masking any such transition, no such extra p_u-values were investigated. Since p_2 was also recorded at all operating points in order to allow plotting of $\bar{p}_{12}$ ($= \bar{p}_1 - \bar{p}_2$) versus $\bar{Q}$, where Q is flow-rate, it was also possible to calculate the value of $\bar{p}_{e2}$ at each point. These data were subsequently used to re-plot the flow-limitation results on top of the previously acquired control-space diagram. On the basis of undeformed tube diameter, flow-rate in ml/s translates approximately to Reynolds number if multiplied by 100.

3. RESULTS

Figure 1 shows the transmural pressure–area curves obtained at eight of the measured locations. The silicone rubber deformation is slightly hysteretic (Bertram 1987); for clarity here only the ascending limb of the measured hysteresis loop is shown in each case. It is seen that there is a progressive change from high compliance between first buckling and opposite wall

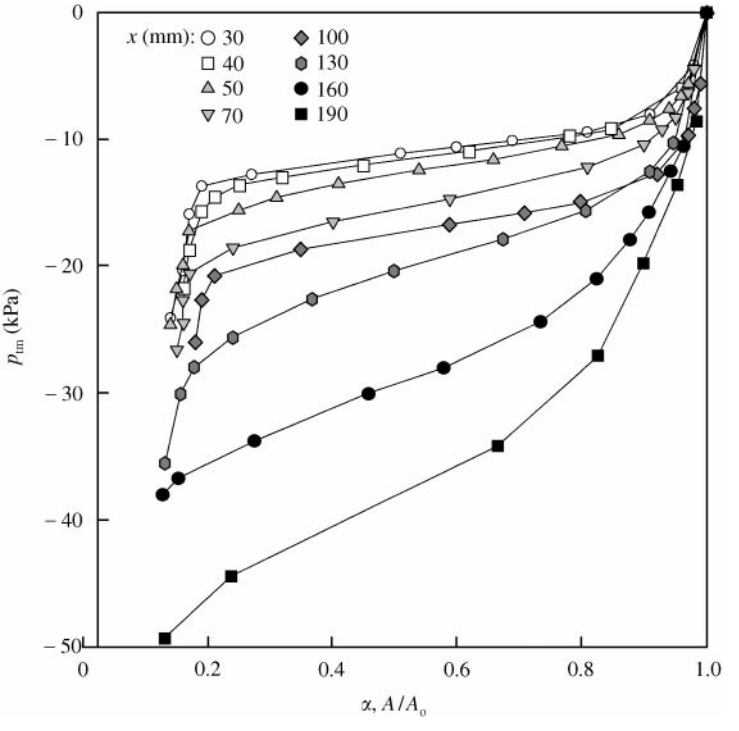

Figure 1. Pressure–area curves measured at eight locations along the tapered-stiffness tube. The origin of axial coordinate x is the upstream end of the unsupported segment of silicone rubber tube. Because the silicone rubber deforms slightly hysteretically, a different path is traced out for each direction of pressure change; for clarity only the ascending limb of the measured hysteresis loop is shown for each case here.

contact (the two knees of the curve) near the thin-walled end of the tube, to lower compliance (a steeper slope) towards the thick-walled end. Normalization of transmural pressure by values of the tube bending stiffness P_k calculated on the basis of the linear wall thickness taper did not collapse the eight curves on top of each other, and is not presented; P_k seemed to vary along the tube rather less than as the cube of the local wall-thickness-to-radius ratio (Shapiro 1977). Conceivable explanations for this behaviour include (i) that the thin-shell assumption underlying the above scaling relation was invalid in the thicker parts of the tube, and (ii) that as the wall thickness decreased, the local bending stiffness became less dominant over the effects of the slight longitudinal tension in the tube, so that the assumption of a local tube law became less and less sustainable towards the thin end of the tube.

Figure 2(a) shows the control-space diagram for the situation of increasing p_c. The interesting part of the diagram is that triangular space between the region at the bottom where the tube is not collapsed at any point, and the region at the top where the tube is flattened along its entire length and only small-amplitude noise-like fluctuations of p_2 are registered. This triangle is defined by boundaries of finite width constituting unattainable zones, where the corresponding value of $\bar{p}_{e2}$ cannot be held because the required value of p_2 is only visited in transit between the regions on either side. Broadly, the space within is divided into two main regions. The upper and larger of these regions corresponds to where the tube is collapsed as far as the downstream end, and the tube throat, where collapse is most intense and oscillations are most vigorous, is immediately upstream, centred 40–50 mm before the downstream end. In this main region occur sub-regions each of which corresponds to an oscillatory mode seen in the uniform tube. The lower region, which we describe as consisting of "weak milking" oscillations, corresponds to tube collapse as far as an intermediate point along the unsupported length. In this region, the throat position was variable and moved noticeably with each cycle of oscillation [hence the term milking (Bertram 1982)]. Upstream of that point, the tube was essentially collapsed over the whole segment from the upstream end, to an extent depending on flow-rate, and the collapsed-tube cross-sectional area was observed to vary slightly along the tube so as to suggest a series of spatial waves. Thus, there were between one and four minima of area along the collapsed segment. Because the oscillations in this whole region were weak (of small amplitude relative to those recorded when the tube is uniform or collapsed to the downstream end) and highly variable, we did not attempt to introduce a conductance catheter to quantify this behaviour.

The corresponding control space for p_e-reduction is shown in Figure 2(b). None of the boundaries were in precisely the same place as when increasing p_e, and some qualitative differences appeared: in particular, a high-frequency (H) region divided off from the low-frequency oscillation region. Within this latter, the various types of low-frequency oscillation merged smoothly into each other. This again is a qualitative difference from the corresponding behaviour in the uniform tube, where unattainable zones marked off the low-frequency modes. A definition of the LU, LD and H modes by way of waveform illustrations was given by Bertram (1986a, figures 8 and 6), and of the LU, LD and MC modes by Bertram *et al.* (1990, figures 6 and 9). The notation DC (double collapse) refers to an oscillation intermediate between the LU mode (one brief collapse per cycle) and the MC mode ("multiple collapse"—multiple pronounced minima of p_2 during the collapse phase), in which the cyclic trough of p_2 comprises just two MC-type minima [not to be confused with the 2/3 mode (Bertram 1986a, figure 10)]. The DC mode, of which an example is shown in Figure 3, was considered MC by Bertram *et al.* (1990). Figure 3 also illustrates some examples of hard-to-classify oscillations. By comparison with the thick-walled uniform tube investigated previously, where oscillation-mode regions distinctly differentiated by

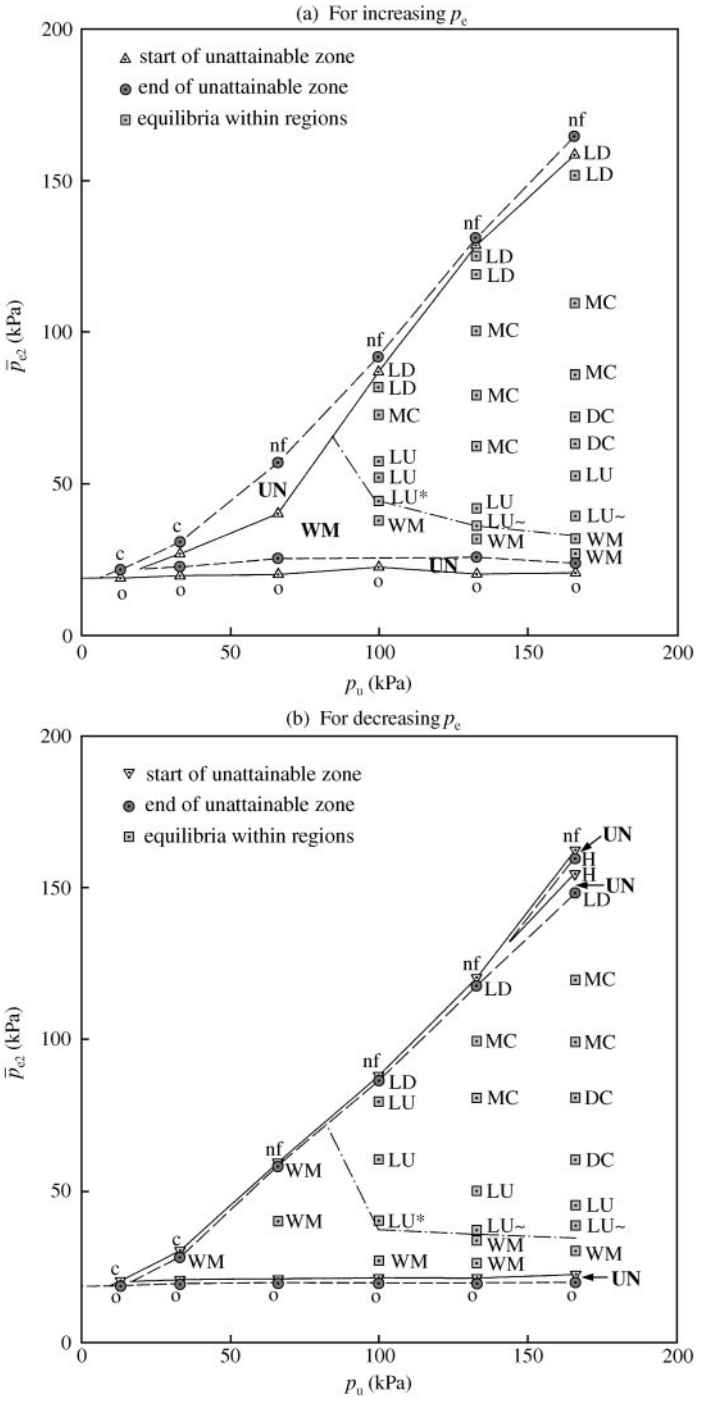

Figure 2. Control-space diagrams for the tapered-stiffness tube when (a) p_e was increased or (b) decreased, to arrive at the value of $\bar{p}_{e2}$ shown. Each operating point is accompanied by an indication of tube behaviour: o = steady flow, open tube; c = steady flow, collapsed tube; UN = unattainable zone; WM = weak (small-amplitude) milking oscillation; LU, LD, DC and MC = large-amplitude low-frequency modes; H = large-amplitude high-frequency mode; nf = small-amplitude noise-like fluctuations (see text for further explanation of some of these terms).

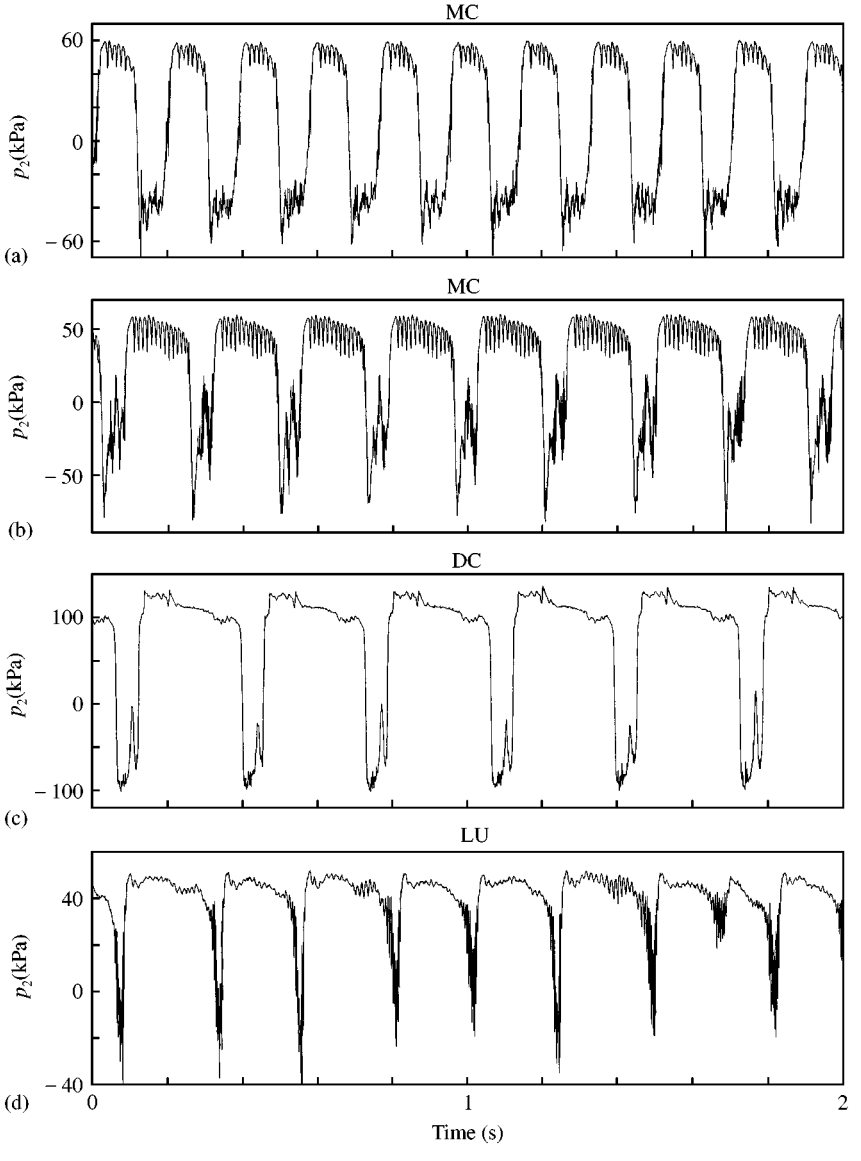

Figure 3. Four examples of large-amplitude low-frequency oscillations, each illustrating where an alternative classification to that adopted is possible. In each case a 2 s window of p_2 is shown. From (a) to (d) the corresponding coordinates in (p_u, $\bar{p}_{e2}$) control space are respectively (100, 86.0), (100, 63.4), (166, 62.1) and (100, 46.3) kPa. Both (a) and (b) show MC (multiple collapse) modes, but in (a) the amplitude of the p_2 oscillations within the waveform trough is marginal; neglecting these would reclassify this example as LD, since the collapse phase occupies half of the cycle. The example (b) would be LU based on collapse-phase duration, but the trough includes multiple pronounced minima (with superimposed very-high-frequency variations). Both (a) and (b) also show pronounced periodic variations (frequency about 89 Hz) during the phase of high p_2; this behaviour was not seen in the uniform thick-walled tube, and appears to be simultaneous W4 oscillation (see below). (c) Example of the DC (double collapse) mode, previously included in the MC category. Many waveform examples were observed which because of marginal trough spike height might be considered either DC or LU. (d) The WM oscillations merged into the LU mode by gradual deepening of the trough; this example, which is classified LU on the basis of peak-to-peak size and brevity of collapse, still retains the superimposed higher frequency and the period and amplitude variability of the adjacent WM region.

waveform shape or abrupt frequency change were prominent, the tapered-thickness tube was characterized by indistinct region boundaries. Abrupt mode changes as p_e was varied, giving rise to unattainable zones (discontinuous changes in $\bar{p}_2$) and hysteresis, were largely absent. Oscillation waveshapes were also somewhat more variable, adding yet further intriguing examples to the menagerie of varieties noted by Bertram *et al.* (1991). The examples in Figure 3, of MC oscillations with pronounced flutter during the noncollapsed phase and of LU oscillation at the edge of the weak milking region, emphasise the difficulty of imposing a systematic categorisation scheme.

Figure 4 shows diagrams of $\bar{p}_{12}$ versus $\bar{Q}$ at a series of constant $\bar{p}_{e1}$-values, for both increasing p_e [Figure 4(a)] and decreasing p_e [Figure 4(b)] as in Figure 2. As in the uniform tube (Bertram and Castles 1999), flow limitation is evident: beyond a value of $\bar{p}_{12}$ that rose slightly as $\bar{p}_{e1}$ was reduced, $\bar{Q}$ no longer increased with $\bar{p}_{12}$. As $\bar{p}_{e1}$ was reduced, a degree of "negative effort dependence" became apparent, i.e. $\bar{Q}$ decreased as $\bar{p}_{12}$ increased. Compared with the corresponding curves for the uniform tube (Bertram and Castles), the former dramatic transition from peak $\bar{Q}$ before the tube collapsed to the start of the flow limitation was essentially absent. The peak $\bar{Q}$ scarcely exceeded the flow-limited $\bar{Q}$, and parts of each flow-limitation curve were instead inhabited by multiple points for each p_u-value, each point constituting a flow-rate satisfying the qualifications for inclusion on this constant-$\bar{p}_{e1}$ curve. The range of $\bar{p}_{e1}$-values that spanned the curves of interest (from a minimum value where the tube never collapsed before the maximum available p_u was reached, to a maximum where the flow-rate was limited at all p_u-values down to the minimum of 13 kPa) was much smaller than in the uniform tube. For the case of increasing p_e, the $\bar{p}_{e1}$-range here was 6–11 kPa [Figure 4(a)]; in the uniform tube it was 30–50 kPa. For p_e-reduction [Figure 4(b)], the tapered-tube range was 3–9 kPa, where in the uniform tube it was 5–26 kPa (noting that the maximum p_u here was 166 kPa, whereas the more robust uniform tube allowed us to go to 200 kPa maximum). This difference is to be expected, because the tapered tube was on average thinner than the uniform tube.

The most profound difference between flow limitation in the uniform thick-walled tube and in the tapered-stiffness tube is that flow limitation in the tapered tube occurred in conjunction with large-amplitude low-frequency oscillation. Operating points in Figure 4(a) are annotated with an indication of behavioural mode; those points on parts of the curves where $\bar{Q}$ was independent of, or diminished with increases in, $\bar{p}_{12}$ include examples of all four sub-divisions of low-frequency waveform type we observed when constructing the control space. Figure 4(b) shows also flow-limited points where the tube exhibited "weak milking" oscillation.

In the case of increasing p_e, Figure 4(a), at the one p_u-value, p_e-adjustment yielded up to six operating points sharing the desired $\bar{p}_{e1}$-value, i.e. the relation between p_e and $\bar{p}_{e1}$ was no longer positive monotonic. Each member of one of these clusters occurred at a different value of both $\bar{Q}$ and $\bar{p}_{12}$. Broken lines join the members of a cluster, and in the case of the simpler curves, where only a couple of points form one cluster (e.g. $\bar{p}_{e1} = 11$ kPa), a solid line joins the rest of the operating points, i.e. links points at the same $\bar{p}_{e1}$ but differing p_u. At $\bar{p}_{e1} = 7$ and 8 kPa, the spread of the points involved in each cluster is such that no such solid line is meaningful. At $\bar{p}_{e1} = 6$ kPa, collapse occurs only at $p_u = 166$ kPa, the highest value explored; a cluster of two points occurs, one of which is not collapsed. At $\bar{p}_{e1} = 5$ kPa, collapse did not occur for any value of p_u up to the maximum used; all points on this curve are overlaid by points on other curves, along the almost horizontal curve-portions at the base of the graph.

The existence of these clusters leads one immediately to conclude that here is an important difference from the flow-limitation behaviour of a uniform collapsible tube,

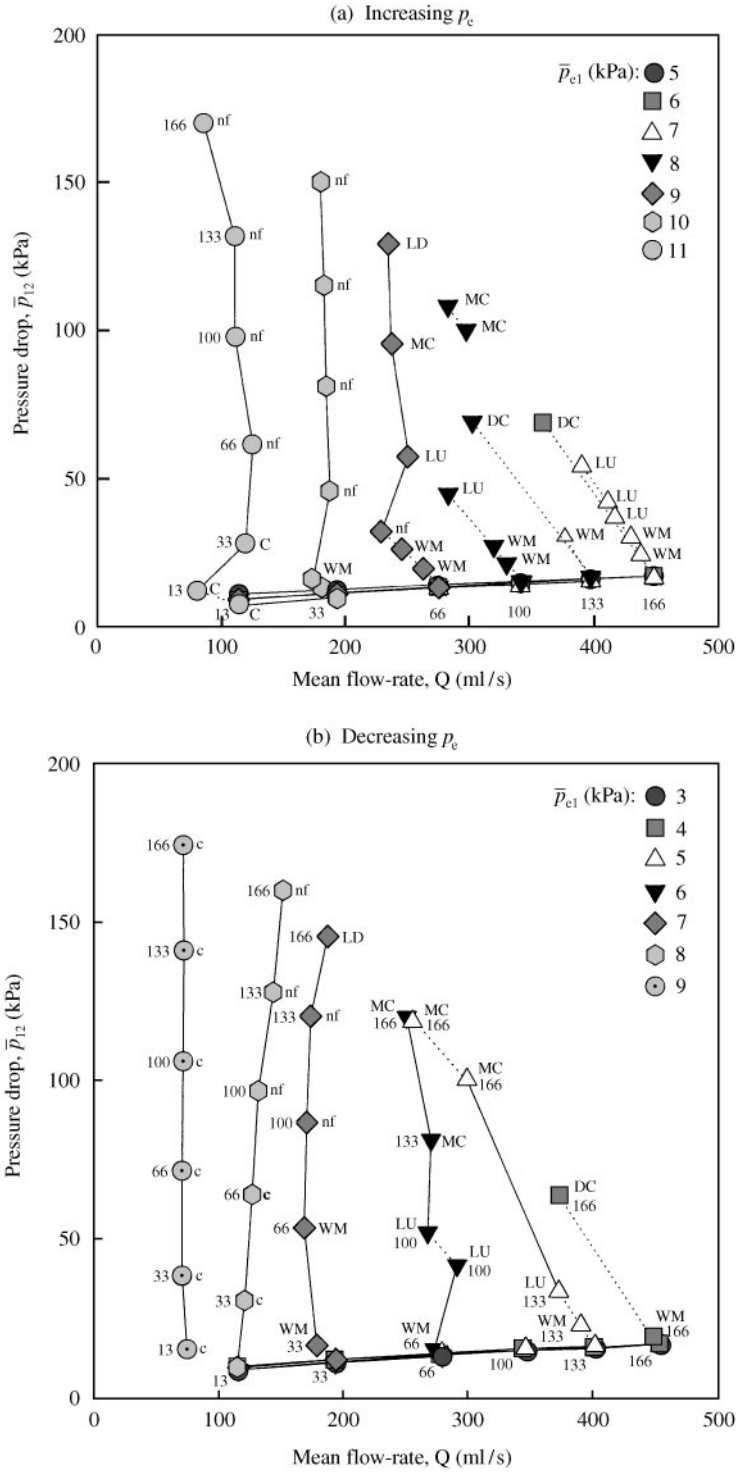

Figure 4. Curves of constant $\bar{p}_{e1}$, showing how pressure drop $\bar{p}_{12}$ and flow-rate $\bar{Q}$ vary as the upstream head p_u is changed. At each point, p_u was set, then p_e was adjusted (a) upwards or (b) downwards to arrive at the $\bar{p}_{e1}$ for that curve. In (b), the value of p_u is shown next to the symbol in every case, as is an indication of the tube behaviour. In (a), the p_u-value is shown for points on the $\bar{p}_{e1} = 5$ and 11 kPa curves only; p_u-values for points on other curves may be deduced from their relative position as in (b).

where the flow-limited $\bar{Q}$ is a monotonic function of $\bar{p}_{e1}$, at least for a given direction of p_e-adjustment, i.e. after taking into account the dynamical system hysteresis. Nonuniqueness of the flow-limited $\bar{Q}$ requires that it be possible to section the figure horizontally at a given $\bar{p}_{12}$-value and find more than one flow-rate for a single $\bar{p}_{e1}$. We have not found a plotting style which both makes it explicit how this is achieved and avoids unduly complicating the figure. Instead, we choose to guide the reader through the construction by eye. For an example, consider the $\bar{p}_{e1}$-value of 8 kPa in Figure 4(a, b), where two points were found at $p_u = 166$ and 133 kPa, and four points were found at 100 kPa. Between 133 and 166 kPa, any p_u-value would give two points. Although the precise locations of these intermediate pairs are not known, we may assume that they lie approximately on the remaining two sides of the quadrilateral of which the two dashed lines shown, joining the two members of the 133-cluster and the two members of the 166-cluster, form opposite sides. Similarly, at some p_u between 133 and 100 kPa, the two points become four, but all may be expected to lie inside or on the borders of a similar quadrilateral. Thus where clusters exist, the single curve at a given $\bar{p}_{e1}$ becomes a series of curves, of which the salient features are given by the values of p_u which were investigated. A horizontal line would then always cut more than one curve in the series, corresponding to nonuniqueness as defined above; these intersections would occur at different p_u-values. Thus the existence of the clusters, while not in itself constituting nonuniqueness in the above sense, because the cluster members occur at differing $\bar{p}_{12}$-values, implies it.

Clusters of two or three operating points all on the one constant-$\bar{p}_{e1}$ curve at a given p_u-value were also present in the case of reducing p_e [Figure 4(b)] for $\bar{p}_{e1}$-values below 8 kPa. Taking as an example the curve for $\bar{p}_{e1} = 6$ kPa, only one operating point was found at $p_u = 133$ kPa, but two were found at $p_u = 100$ and at 66 kPa. The routing of the solid lines to one rather than the other member of the pair of points at each of these p_u-values shows the order in which the points were found as p_e was reduced. Intermediate p_u-values were not explored; thus the clustering, which implies splitting of the $\bar{p}_{e1}$-curve, began at a p_u value between 133 and 100 kPa and persisted for all p_u-values down to that at which flow limitation and tube collapse ceased. At lower values of $\bar{p}_{e1}$ than 6 kPa, two or three operating points sharing the same $\bar{p}_{e1}$ were found at all p_u-values where flow limitation occurred.

Bertram & Castles showed, by plotting the results of such flow-limitation experiments on control space, that when, whilst increasing p_u in steps and at each step manipulating p_e so as to regain the same value of $\bar{p}_{e1}$, the tube collapsed, the following transition to where $\bar{Q}$ was independent of $\bar{p}_{12}$ crossed over all of the oscillatory regions. This constituted an explanation of why the self-excited oscillations which are normally so noticeable a feature of collapsible-tube behaviour at substantial Reynolds number did not occur during flow limitation. Figure 5 shows similarly the results from each panel of Figure 4 plotted on top of the corresponding control space from Figure 2. In the uniform tube, all the flow-limited operating points lay in the c- or nf-mode regions. In the tapered-stiffness tube by contrast, while some of the flow-limitation curves still occupy that position, others inhabit the large-amplitude oscillation regions [increasing p_e, Figure 5(a)] or both the large-amplitude and weak milking regions [reducing p_e, Figure 5(b)].

Figure 6 shows explicitly that $\bar{p}_{e1}$ depended nonmonotonically on p_e when p_e was increased. The most prominent reverse curvature occurs at the highest value of p_u. While the tube was open, $\bar{p}_{e1}$ increased with p_e. Not all of this trivial part of the relation is shown, but it would extend the almost vertical line of "open" tube points as in the case of $p_u = 100$ kPa. A horizontal line anywhere between $\bar{p}_{e1} = 3.6$ and $\bar{p}_{e1} = 5.2$ kPa would then cut the $p_e/\bar{p}_{e1}$ relation for $p_u = 166$ kPa in three places. Lesser but non-negligible non-monotonic dependence occurred at the other p_u-values. At $p_u = 166$ kPa, the range where a given $\bar{p}_{e1}$ resulted

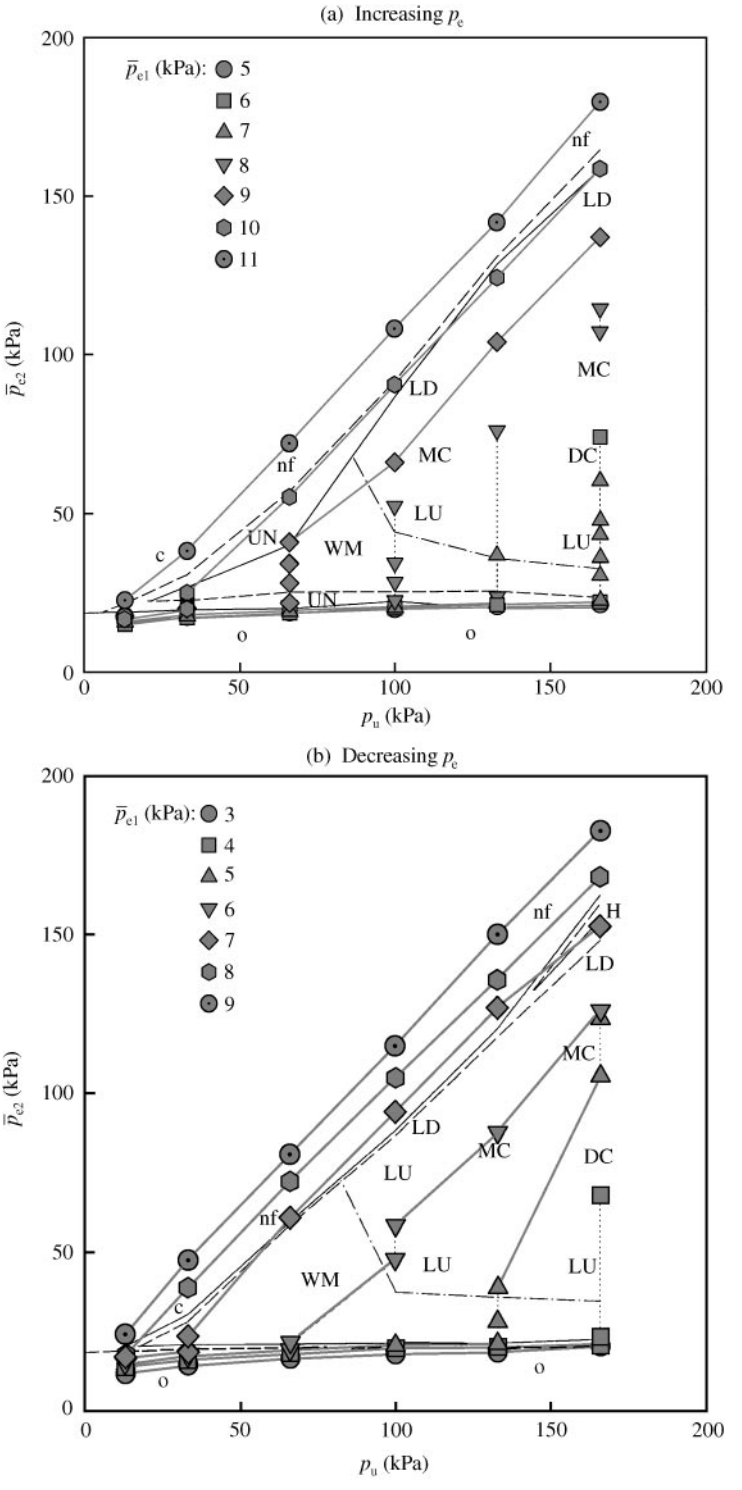

Figure 5. The constant-$\bar{p}_{e1}$-curve data from Figure 4(a) and 4(b), re-plotted here in (a) and (b), respectively, in terms of their (p_u, $\bar{p}_{e2}$)-coordinates, on top of the control-space diagrams of Figures 2(a) and 2(b), respectively. For clarity, the individual data points from Figure 2 are suppressed, and only the general behaviour in each region of control space is indicated. Similarly, the individual behaviour annotations for the Figure 4 data points are omitted, but can be discovered by comparison with Figure 4.

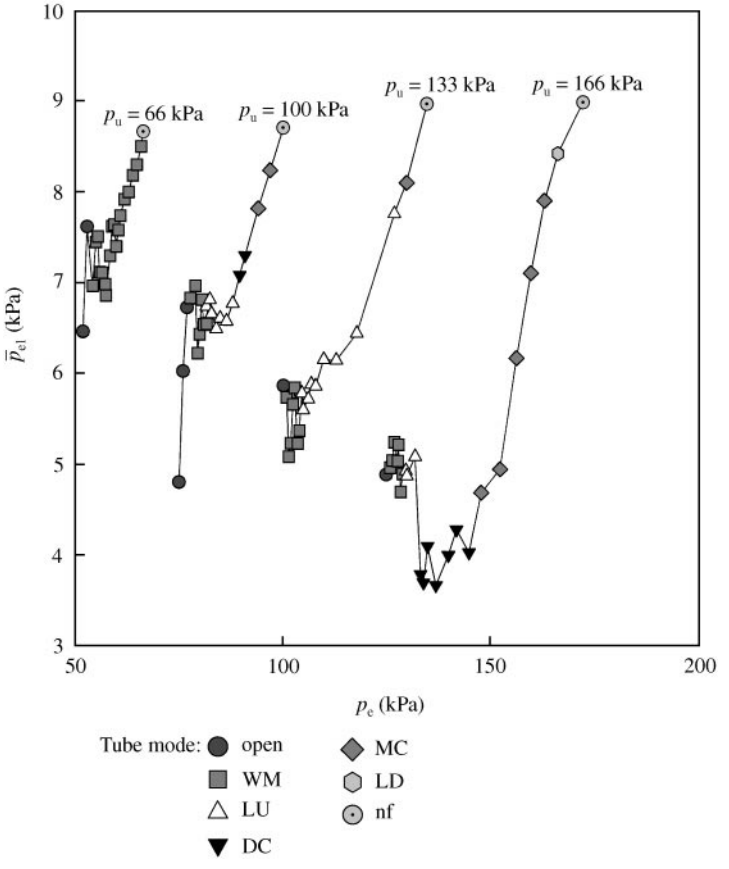

Figure 6. The variation of $\bar{p}_{e1}$ with p_e when p_e was increased, at four constant values of upstream head p_u. Each curve starts with the tube open, then the "nf" state is reached via a variable number of other modes *en route*.

from more than one p_e involved the tube being first open, then collapsed and oscillating, initially in the weak milking mode, then successively in the low-frequency large-amplitude styles LU, DC and MC. At $p_u = 66$ kPa, the multiply-valued range involved only the open tube and the weak milking mode. At $p_u = 100$ and 133 kPa, the range involved the open tube and the weak milking and LU modes.

All of the data for each curve in Figure 6 were obtained by incrementing p_e while keeping p_u constant. This is a different procedure from that used to create Figure 4, where each curve follows a desired value of $\bar{p}_{e1}$, and p_u was reset for each point before using p_e to re-attain $\bar{p}_{e1}$. Figure 7 shows the data from Figure 6 plotted on the same axes of $\bar{Q}$ and $\bar{p}_{12}$ as Figure 4. This is a traditional way to plot collapsible-tube data, popularized by Conrad (1969). Note however that the non-unique dependence of $\bar{Q}$ on $\bar{p}_{e1}$ is missed in this presentation. Figure 8 shows the non-unique $\bar{Q}/\bar{p}_{e1}$ relation explicitly, separating the curves for different values of p_u so that their overlap does not obscure detail of the reverse curvature. As explained above in the context of Figure 4, the existence of multiple flow-rates for a given $\bar{p}_{e1}$ and p_u entails the same number of multiple solutions for flow-rate at a given $\bar{p}_{e1}$ and $\bar{p}_{12}$, these being the variables experienced by the tube.

Figure 9 shows the equivalent results for the case of p_e-reduction, but now on the one set of axes so that comparison can be made between the results obtained at different p_u-values. Initially (at high p_e), the tube was collapsed along its entire length. As p_e was decreased,

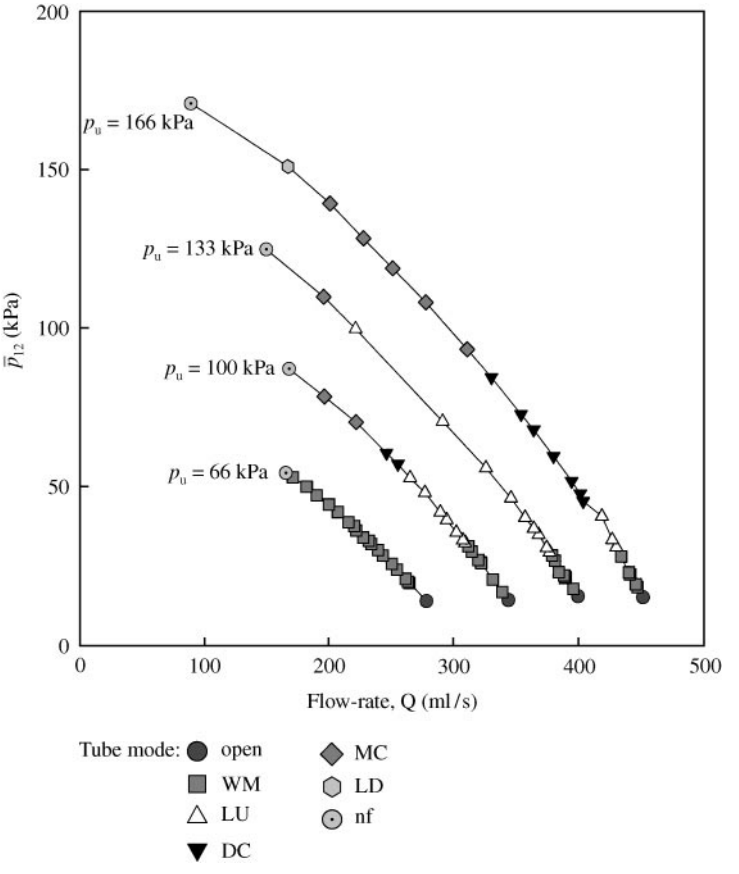

Figure 7. The data of Figure 6, re-plotted in terms of their $(\bar{Q}, \bar{p}_{12})$-coordinates, again with symbols indicating the mode of tube behaviour at each point as p_e was increased while keeping p_u constant.

small-amplitude noise-like fluctuations (nf mode) occurred, then gave way to large-amplitude low-frequency modes. In general, Figure 9 shows a single inverse relationship between $\bar{Q}$ and $\bar{p}_{e1}$ which prevails irrespective of collapsed mode and p_u-value (the extent of the $\bar{p}_{e1}$ discrepancy between the four curves at, say, $\bar{Q} = 200$ ml/s was of the same order as the curve reproducibility error 1/m – result not shown). Once p_e was insufficient for tube collapse, $\bar{Q}$ of course became dependent on p_u and independent of $\bar{p}_{e1}$.

The nonmonotonic dependence of p_{e1} on p_e shown in Figure 6 also occurred when p_e was being reduced, and was again minor except at the highest p_u-value. It is important to note that a non-monotonic $\bar{p}_{e1}/p_e$-relation, while here leading to nonunique dependence of $\bar{Q}$ on $\bar{p}_{e1}$ at a given $\bar{p}_{12}$, is not guaranteed always to entail such flow-limited flow-rate multiplicity. This question will be pursued in further work.

3.1. Weak Milking Oscillations

Figure 10 shows a control-space diagram representing the results of the separate experiments we carried out to observe in detail the weak milking region. Both increasing and decreasing p_e were investigated, but the diagram is for the case of reducing p_e. The WM region comprises four distinct types of oscillation, each of which is shown in Figure 11; in the legend to Figure 10, they are labelled W1–W4. The control-space diagram does not

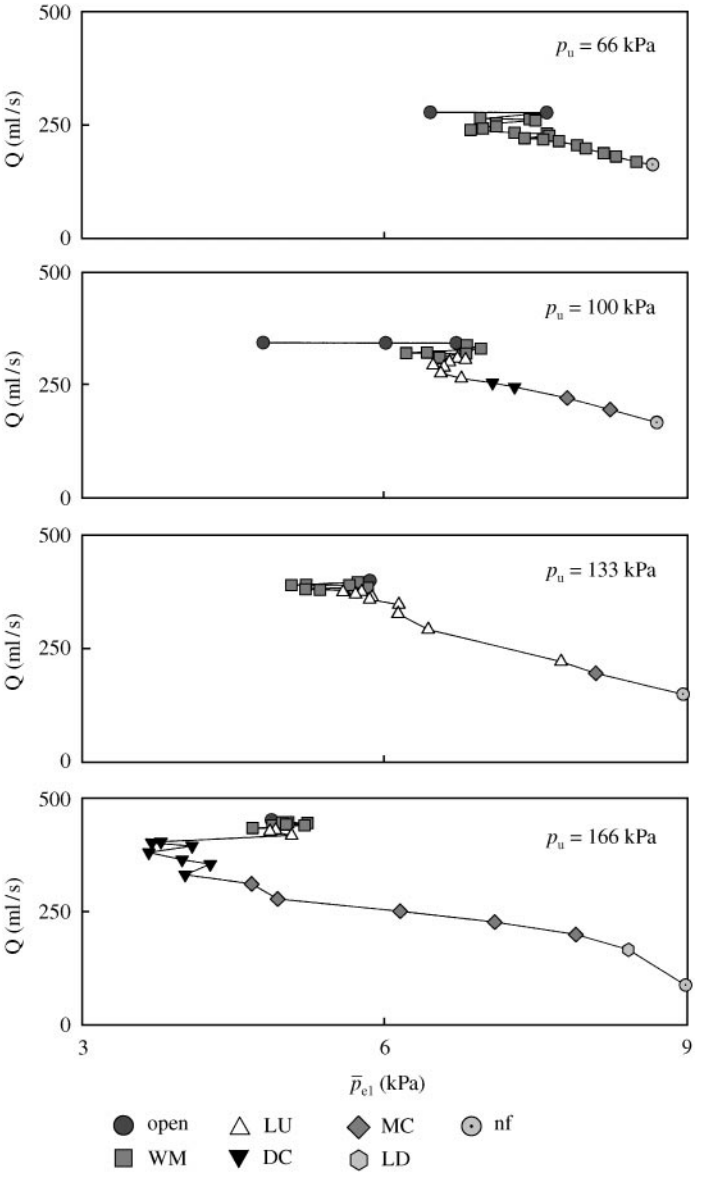

Figure 8. The data of Figures 6 and 7, now plotted to show how $\bar{Q}$ varied with $\bar{p}_{e1}$.

show boundaries between the sub-regions of WM-space occupied by each of the four waveform types, because we could not discern any discontinuity in $\bar{p}_{e2}$ at the change-overs between modes. It was found that with very few exceptions the range of $\bar{p}_{e2}$-values where each W mode was seen was independent of the direction of p_e-change. Thus, hysteresis did not play a large role in setting the dynamics when the tube throat was away from the downstream end of the tube. Modes W1–W3 were distinguished not only by waveform shape, but also by how many minima of tube area (1–3, respectively) were present along the collapsed section of the tube. Up to four or perhaps five minima were just discernible occasionally at the WM/LU boundary. These standing waves of area are possibly similar to those observed by Kececioglu *et al.* (1981). Mode W4 in some ways resembled the

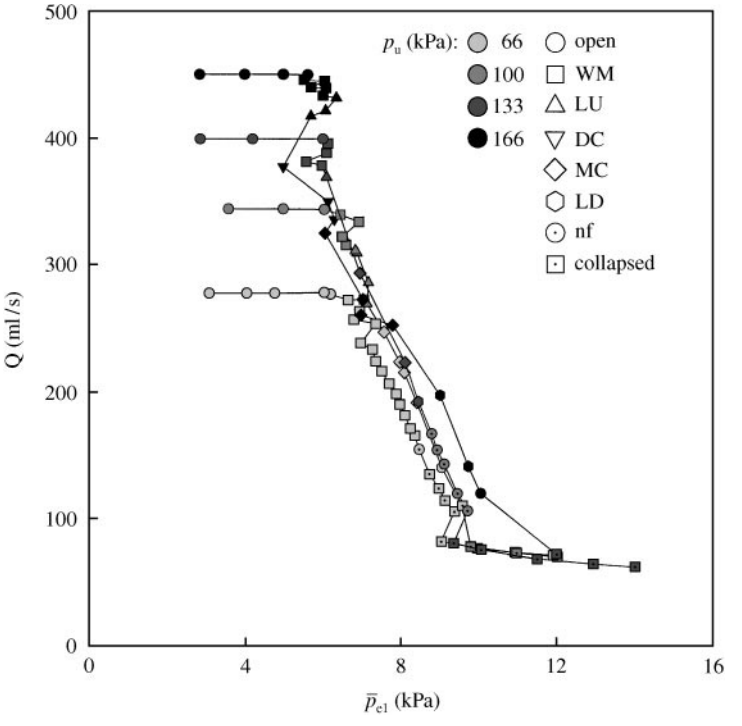

Figure 9. As Figure 8, but now for the case of incremental p_e *reduction* while holding a single value of p_u. With the four curves overlaid on one set of axes, it is seen that overall there is a single p_u-independent relation between $\bar{p}_{e1}$ and $\bar{Q}$ except when the tube is not collapsed at all (○). However, as in Figure 8, there are lesser portions of each curve which double back on themselves, showing a nonmonotonic dependence of $\bar{Q}$ on $\bar{p}_{e1}$.

high-frequency (56 Hz) oscillation labelled H in Figure 2(b); the frequency (around 80 Hz) was of the same order, and the tube was collapsed along essentially its whole length. However, as can be seen in Figure 11, the peak-to-peak p_2-amplitude of the oscillation (30 kPa) was only a little larger than that of the other WM-region oscillations, whereas the equivalent amplitude of the H oscillation in Figure 2(b) was some 180 kPa.

The description of modes W1–W3 in terms of standing waves neglects the substantial axial motion of the throat position(s) during the oscillation. Typically, the W1 throat (point of maximum collapse and minimum area) oscillated in the range $x = 70$–100 mm, the W2 minima in the ranges 60–80 and 110–140 mm, and the W3 minima in the ranges 55–75, 105–125 and 155–180 mm, where $x = 0$ is the upstream end of the unsupported tube. Four minima would occupy time-average positions between 60 and 190 mm. When three or four minima were present, in some cases the penultimate one would be almost stationary, while those on either side oscillated axially.

4. DISCUSSION

As noted with respect to Figure 9, finite reproducibility error must be considered in interpreting these data. The sources of this were discussed by Bertram and Castles (1999); they include the ageing and fatiguing of the tube material, imperfect control of circulating fluid temperature and hence viscosity, and pressure transducer deficiencies, including drift, nonlinearity and hysteresis, all of which are magnified when measuring small differences between two large quantities. Repeating the experiment leading to the results for $p_u = 100$

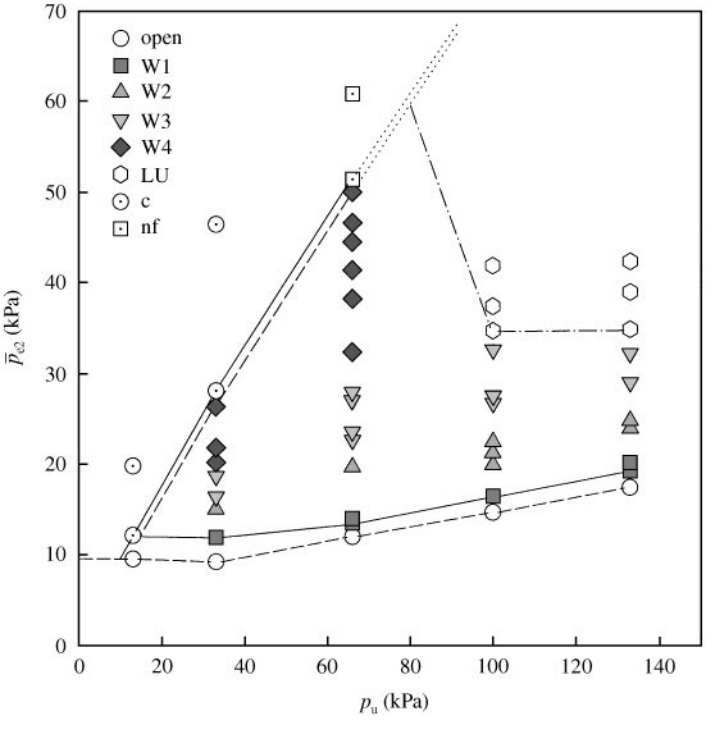

Figure 10. Four WM-region oscillation modes were found; their ranges in $(p_u, \bar{p}_{e2})$ control space are here shown in an enlarged control-space diagram for the case of reducing p_e.

and 166 kPa presented in Figure 9 revealed that while the shape of the curve was largely maintained, offsets in $\bar{p}_{e1}$ of up to $\pm$ 0.6 kPa occurred. Exactly such comparison of different experiments is involved in the overlay of flow-limitation data on control space as in Figures 5(a) and 5(b), and likewise Figures 2(a), 6 and 7 are composed of curves from more than one experiment. Nevertheless, we are confident that all of the conclusions we draw from our results, which are ultimately qualitative, are independent of these experimental factors. Another potential source of reproducibility error would be inability to remount the tube on the rigid pipes at each end in precisely the same way after removal; however, all results reported here were obtained from one tube which was left mounted throughout. An example of changes in control space arising from this factor was given by Bertram *et al.* (1991, cf. figures 4c and 4d).

The study of tapered-stiffness collapsible tubes was initiated by Shapiro (1977), who in the context of a 1-D theoretical model suggested longitudinal variation in wall bending stiffness via thickness variation as one of a number of ways to achieve transition to supercritical flow, where the fluid-flow speed averaged over the cross-section, $\bar{Q}/A$, exceeds c, the pressure-wave speed. Experimental study of such tubes was reported by Kamm *et al.* (1991), arising out of a Master's thesis by Jaekle (1987). The aim was to investigate whether theoretically predicted alternatives to the usual elastic jump from super- to subcritical flow along the tube could be produced experimentally. The flow was aqueous, and the 12·7 mm-i.d. latex rubber tube tapered from 0·4 to 1·5 mm wall thickness over a distance of 210 mm. No evidence of multiple flow-limited flow-rates was found, albeit this question was not the goal of the experiments.

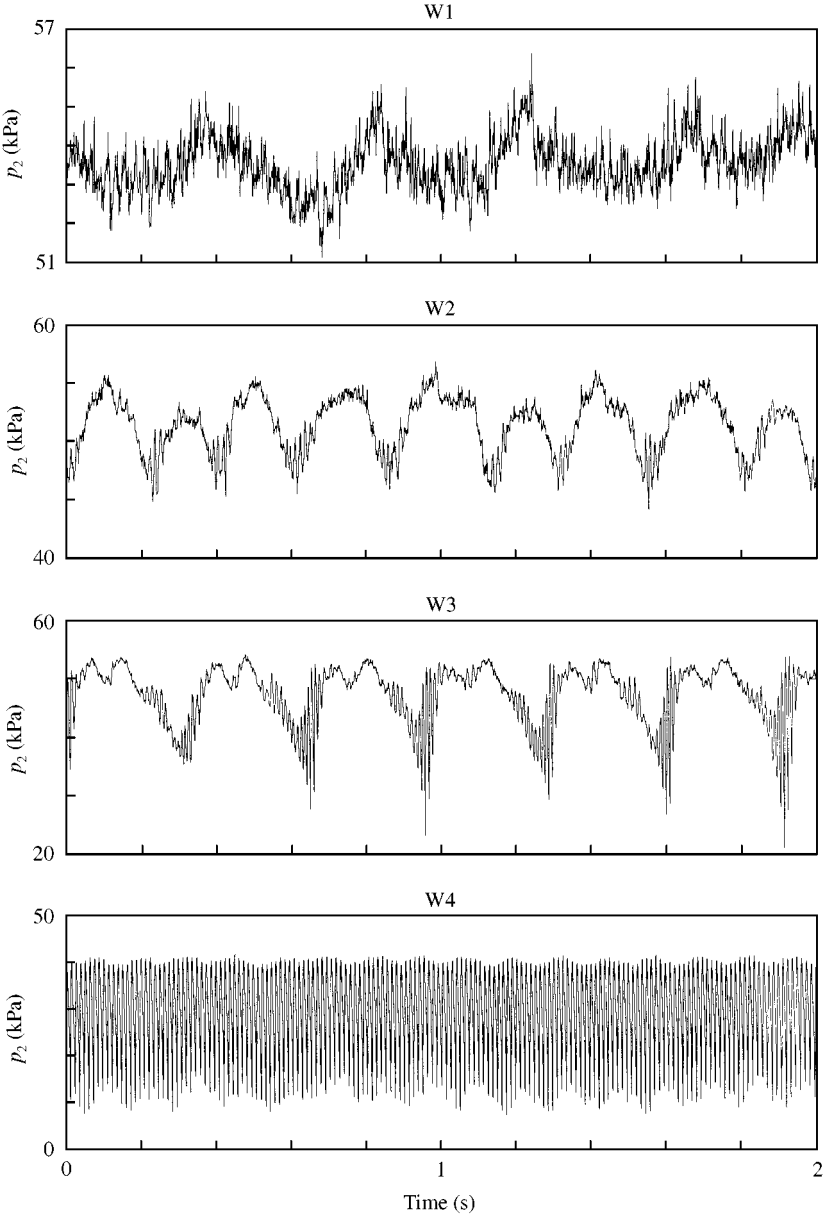

Figure 11. Waveforms for the four WM-region waveform types observed, here labelled W1–W4. The corresponding coordinates in (p_u, $\bar{p}_{e2}$) control space are, respectively, (100, 25·2), (100, 27·8), (100, 33·4) and (66, 29·0) kPa.

Because of interest in the pulmonary applications, air flow through a tapered-stiffness tube was investigated by Patel (1993) and Kamm *et al.* (1993). The tube was silicone rubber of i.d. 12·8 mm, and tapered from 1·3 to 4·5 mm wall thickness over 170 mm. The pressure/flow results indicated that "the flow rate is non-unique in that several different time-mean flows can be generated for a single pair of transmural pressure values". (The pair in question was the values at the ends, $\bar{p}_{e1}$ and $\bar{p}_{e2}$; several meant up to three.) Unfortunately, these intriguing observations have not been followed up in detail. Microphone

recordings were made of tube flutter, typically at 80–150 Hz, with peak spectral power at the second, third or fourth harmonic; broad-band oscillations were also observed.

Most recently, Ohba *et al.* (1998) reported pressure-flow results from experiments on a tapered-stiffness tube at the same conference as saw the first presentation of the present results. The tube was of i.d. 5·7 mm, and the wall thickness increased from 0·2 to 1·15 mm over a distance of 40 mm. They observed small-amplitude oscillations associated with a tube throat located in the middle of the tube, and remarked on the absence of the much larger "spike-like" oscillations that they had seen in a uniform tube. It would seem that their small-amplitude oscillations correspond to our region of weak milking, suggesting that had they pursued higher flow-rates and larger external pressures, they would probably have observed, as we did, the throat revert to the downstream end of the tube, and the oscillations to the large spike-like mode (LU in our classification).

Thus, the observations here constitute the first evidence of nonunique dependence of the flow-limited flow-rate on the upstream transmural pressure (excluding the discrepancy due to hysteresis between the relationship for increasing and for decreasing external pressure noted by Bertram and Castles in uniform tubes) for collapsible tubes conveying an aqueous flow. The extent of the nonuniqueness is minor relative to that found by Kamm *et al.* (1993) for air flow; here, the variation in flow-rate between points having the one value of upstream transmural pressure, after excluding those where the tube was not collapsed, was no more than 17%; if the comparison were made at the one value of tube pressure drop, the variation would be less. In contrast, Patel (1993) observed in one case flow-rates of 0·8, 1·8 and 2·5 l/s (spanning an estimated Reynolds number range of 5000–16 000). Since the present experiments involve only aqueous flow, Patel's thesis observations remain in need of confirmation.

Besides this nonuniqueness, there are other major qualitative differences from the behaviour of otherwise similar uniform tubes. To reiterate, the uniform tubes examined by Bertram and Castles exhibited nonoscillatory flow limitation, excluding small-amplitude noise-like fluctuations ("nf" mode) and one small region of 22 Hz oscillation. The peak flow-rate was several times the flow-limited flow-rate at the smallest negative value of upstream transmural pressure, the two states being linked by an oscillatory transition. Moreover, the relation between flow-rate and upstream transmural pressure was monotonic for a given direction of external pressure change. By contrast, the tapered-stiffness tube here had (i) flow limitation straddling regions of control space corresponding to large-amplitude oscillation as well as nonoscillatory regions, (ii) an absence of the distinct transition to or from flow limitation involving sharp changes in flow-rate and (iii) in many cases multiple flow-limited flow-rates. The oscillatory regions were expanded by the addition of the region of complex weak milking modes. These modes were of small amplitude relative to the above modes, and corresponded to states where the tube throat was remote from the downstream end of the unsupported segment of tube.

The fact that these differences are qualitative, not simply quantitative, needs emphasis because the tapered-stiffness tube, having been created by removal of material from a segment of the uniform tube with which it is here compared, was on average less stiff. Consequently, the differences noted in the Results section in the ranges of upstream transmural pressure over which the change-over occurred, from no collapse at any upstream pressure to collapse and flow limitation at all upstream pressures used, are of very limited significance. It is not easy to define the uniform tube constituting the most appropriate comparison for the tapered-stiffness tube; different comparison parameters would suggest different values of uniform wall thickness. Another approach would be to examine the behaviour of a tube having uniformly the minimum wall thickness of the tapered tube; such a tube together with that observed by Bertram and Castles would

straddle the average stiffness of the present tube. Such an additional investigation is planned for a forthcoming paper.

With reference to pulmonary applications, one may speculate on the relation between the oscillatory flow limitation found here (but not in the uniform tube) and lung wheezing sounds during a maximal forced expiration. A host of parameter differences between these experiments and the pulmonary airways, most notably the use of water instead of air, mean that only a qualitative analogy can be made. The results from the uniform tube led Bertram and Castles to the conclusion that lung wheezing must be the product of either what in the context of their experiments was small-amplitude noise-like fluctuations of the pressure downstream ("nf" mode), or large-amplitude oscillation from the transition as each segment of airway left flow limitation, while the flow-limited site travelled upstream. The results from the tapered-stiffness tube suggest that either small-amplitude noise-like fluctuations or large-amplitude periodic oscillations could be emitted from the flow-limited airway site itself. The apparently inadequate frequency of the large-amplitude oscillations recorded here, for emulating audible lung wheezing, is a consequence of the dense fluid in use here; much higher frequencies would result from the use of air, without any other parameter change. However, what necessarily changes vastly at the same time is the wall mass relative to the fluid mass [the most appropriate quantity to characterize this idea is the ratio of the densities times the ratio of wall thickness to radius; see Luo and Pedley (1998)]. This means that the mechanism of collapsible-tube air-flow-induced oscillation can be different from that which produces aqueous-flow-induced oscillations. Flutter is an appropriate term for the most likely mode when air is the fluid (Grotberg and Gavriely 1989; Walsh 1995).

ACKNOWLEDGEMENTS

W.C. was supported by a grant from the Australian Research Council. C.D.B. thanks Professor R.D. Kamm for advice on many aspects of these experiments.

References

Bertram, C. D. 1982 Two modes of instability in a thick-walled collapsible tube conveying a flow. *Journal of Biomechanics* **15**, 223–224.

Bertram, C. D. 1986a Unstable equilibrium behaviour in collapsible tubes. *Journal of Biomechanics* **19**, 61–69.

Bertram, C. D. 1986b An adjustable hydrostatic-head source using compressed air. *Journal of Physics E, Scientific Instruments* **19**, 201–202.

Bertram, C. D. 1987 The effects of wall thickness, axial strain and end proximity on the pressure-area relation of collapsible tubes. *Journal of Biomechanics* **20**, 863–876.

Bertram, C. D. & Butcher, K. S. A. 1992 A collapsible-tube oscillator is not readily enslaved to an external resonator. *Journal of Fluids and Structures* **6**, 163–180.

Bertram, C. D. & Castles, R. J. 1999 Flow limitation in uniform thick-walled collapsible tubes. *Journal of Fluids and Structures* **13**, 399–418.

Bertram, C. D. & Godbole, S. A. 1995 Area and pressure profiles for collapsible tube oscillations of three types. *Journal of Fluids and Structures* **9**, 257–277.

Bertram, C. D., Raymond, C. J. & Pedley, T. J. 1990 Mapping of instabilities for flow through collapsed tubes of differing length. *Journal of Fluids and Structures* **4**, 125–153.

Bertram, C. D., Raymond, C. J. & Pedley, T. J. 1991 Application of dynamical system concepts to the analysis of self-excited oscillations of a collapsible tube conveying a flow. *Journal of Fluids and Structures* 5, 391–426.

Bertram, C. D., Sheppeard, M. D. & Jensen, O. E. 1994 Prediction and measurement of the area-distance profile of collapsed tubes during self-excited oscillation. *Journal of Fluids and Structures* **8**, 637–660.

BROWER, R.W.& SCHOLTEN, C. 1975 Experimental evidence on the mechanism for the instability of flow in collapsible vessels. *Medical and Biological Engineering* **13**, 839–845.

CONRAD, W. A. 1969 Pressure-flow relationships in collapsible tubes. *IEEE Transactions on Bio-Medical Engineering* **16**, 284–295.

GAVRIELY, N., SHEE, T. R., CUGELL, D. W. & GROTBERG, J. B. 1989 Flutter in flow-limited collapsible tubes: a mechanism for generation of wheezes. *Journal of Applied Physiology* **66**, 2251–2261.

GRIFFITHS, D. J. 1969 Urethral elasticity and micturition hydrodynamics in females. *Medical and Biological Engineering* **7**, 201–215.

GROTBERG, J. B. & GAVRIELY, N. 1989 Flutter in collapsible tubes: a theoretical model of wheezes. *Journal of Applied Physiology* **66**, 2262–2273.

JAEKLE, D. E. JR. 1987 Critical transitions associated with steady flow in collapsible tubes with varying wall stiffness. S. M. thesis, Massachusetts Institute of Technology.

KAMM, R. D., ELAD, D., JAEKLE, D. E. JR. & SHAPIRO, A. H. 1991 Theory and experiments on smooth transitions through the critical state ($S = 1$) in collapsible tube flow. 1991 *Advances in Bioengineering*, ASME BED-vol. 20, pp. 329–332.

KAMM, R. D., PATEL, N. R. & ELAD, D. 1993 On the effect of flow-induced flutter on flow rate during a forced vital capacity maneuver. *FASEB Journal* **7**, A11.

KECECIOGLU, I., MCCLURKEN, M. E., KAMM, R. D. & SHAPIRO, A. H. 1981 Steady, supercritical flow in collapsible tubes. Part 1. Experimental observations. *Journal of Fluid Mechanics* **109**, 367–389.

LUO, X. Y. & PEDLEY, T. J. 1998 The effects of wall inertia on flow in a two-dimensional collapsible channel. *Journal of Fluid Mechanics* **363**, 253–280.

MCCLURKEN, M. E. 1978 Shape-independent area measurement in collapsible tubes by an electrical impedance technique. *Proceedings of the 31st Annual Conference on Engineering in Medicine and Biology*, Atlanta GA, p. 95.

OHBA, K., SAKURAI, A. & MAEKAWA, K. 1998 Characteristics of the flow in collapsible tube with continuously varying compliance along the tube axis—its application to extracorporeal circulation. In *Abstracts of the 3rd World Congress of Biomechanics*, Sapporo, Japan, 2–8 August (eds. Y. Matsuzaki *et al.*), p. 38.

PATEL, N. R. 1993 A study of flow limitation and flow-induced oscillations during airflow through collapsible tubing. B.S. thesis, Massachusetts Institute of Technology.

SHAPIRO, A. H. 1977 Steady flow in collapsible tubes. *ASME Journal of Biomechanical Engineering* **99**, 126–147.

WALSH, C. 1995 Flutter in one-dimensional collapsible tubes. *Journal of Fluids and Structures* **9**, 393–408.

YAMANE, T. & ORITA, T. 1992 Self-excited oscillations with and without supercritical flow in collapsible tubes. *Proceedings of the 7th International Conference on Biomedical Engineering*, Singapore, 2–4 December, pp. 502–504.